Effect of O_2 on Selective Catalytic Reduction of NO by C_3H_6 over Fe Catalysts Supported on Porous Clay Heterostructures (Fe-PCH)

Yuan M[1], Ning S[1], Su Y[1]*, Deng W[1] and Zhou H[2]

[1]School of Environmental Science and Engineering, Donghua University, China

[2]School of Intelligent Manufacturing, Changzhou Institute of Engineering Technology, China

*Corresponding author: Yaxin Su, School of Environmental Science and Engineering, Donghua University, Shanghai 201620, China, Tel: +86-21-67792552; Fax: +86-21-67792522; Email: suyx@dhu.edu.cn

Abstract

K10 montmorillonite was used as the raw clay to prepare porous clay heterostructures (PCH) by organic template intercalation and tetraethylorthosilicate (TEOS) was used as silicone source. Fe was load on the PCH support by impregnation method to prepare Fe-PCH catalysts. The catalytic activity tests were carried out in a fixed bed micro-reactor in the atmosphere of 0.1% C_3H_6, 0.1%NO, 0~10%O_2 in N_2 balance. The total flow rate was 100ml/min and corresponding gas hourly space velocity (GHSV) was 15000h^{-1}. The mircro-reaction pathways were studied by Diffuse Reflection Infrared Fourier Transform Spectrometer (DRIFTS). The influence of O_2 on the SCR-C_3H_6 reactivity over Fe-PCH was analyzed. The results showed that Fe-PCH catalyst exhibited the best catalytic performance without oxygen, which reached the maximum NO conversion of 100% at 400^{0}C. When the concentration of O_2 is below a critical value, $[O_2]_{crit}$, the catalytic activity gradually decreased with the increasing concentration of O_2. When the concentration of O_2 is above $[O_2]_{crit}$, the NO conversion was only 20%~30%. Fe-PCH catalysts were characterized by transmission electron microscope (TEM), N_2 adsorption/desorption and X-ray photoelectron spectroscopy (XPS) techniques. The results showed that Fe-PCH had supermicroporous and mesoporous structures. The active components on Fe-PCH catalyst were mainly α-Fe_2O_3 nanorods, exposing (024) and (104) planes. The in situ DRIFTS technique was used to detect the reactive intermediates over the surface of Fe-PCH catalyst, which could help analyze the mechanism of the influence of oxygen on catalytic activity. The results presented that oxygen could inhibit the formation of isocyanate species over Fe-PCH catalyst during C_3H_6-SCR, which might be the reason for the decrease of NO conversion. Finally, a reasonable reaction path of C_3H_6-SCR over Fe-PCH catalyst was proposed.

Keywords: Fe-PCH; Selective catalytic reduction; C_3H_6; NO; DRIFTS

Introduction

Selective catalytic reduction of NO with hydrocarbon (SCR-HC) technology is a new type of flue gas denitrification technology with great application value and development potential. It has received extensive attention in recent years, and the effective catalysts is the core of research. At present, a variety of catalysts that can be applied to HC-SCR technology

have been reported, including metal oxides, molecular sieves, precious metal catalysts, etc. [1,2]. In addition, the advantages of pillared clay catalysts, such as good microporous structure and ion exchange properties, have also attracted the attention of researchers. In 1995, Yang and Li [3] reported for the first time that TiO_2-pillared montmorillonite supported Cu (Cu-TiO_2-PILC) catalysts could catalyze C_2H_4 to reduce NO. Since then, the HC-SCR catalytic performance of a large number of

Effect of O_2 on Selective Catalytic Reduction of NO by C_3H_6 over Fe Catalysts Supported on Porous Clay Heterostructures (Fe-PCH)

Pet Petro Chem Eng J

pillared clay catalysts has been reported successively [4-12]. Recently, Qian, et al. [13] found that Fe-Al-PILC-type pillared clay catalysts can efficiently catalyze the reduction of NO with C_3H_6, and the NO conversion rate can be close to 90% at 350°C. Dong, et al. [14] subsequently reported the results of C_3H_6-SCR on Fe-TiO_2-PILC catalysts under oxygen-enriched conditions. Li Qiancheng, et al. [15] prepared Fe_2O_3 pillared clay (Fe-PILC) by ion exchange method which also had good C_3H_6-SCR catalytic performance. Porous clay heterostructures (PCHs) are a new type of clay-based inorganic functional materials with regular three-dimensional pore structure, first reported by Galarneau, et al. in Nature in 1995 [16]. Compared with traditional pillared clays (PILCs), PCHs can form ordered mesoporous channels between layers through organic template intercalation method, which can improve the adsorption and diffusion rate of reactive gases, which has an important impact on gas-phase catalytic reactions. In addition, the hydrophobic SiO_2 channel walls formed by the organosilicon source endow the PCHs with better hydrothermal stability. The previous experimental results showed by Yuan M, et al. [17] that the Fe-modified PCH catalyst (Fe-PCH) prepared by the impregnation method can catalyze C_3H_6 to reduce NO with an efficiency of 96% at 400°C.

The oxygen concentration has a great influence on the HC-SCR catalytic performance of the pillared clay catalysts. Valverde, et al. [18] found that Cu-TiO_2-PILC has no catalytic activity under oxygen-free conditions, and the addition of a small amount of O_2 is beneficial to improve the C_3H_6-SCR reaction performance of the catalyst; with the increase of oxygen concentration, the maximum NO conversion rate increases first and then decreases. Lin, et al. [19] studied the effect of oxygen concentration on the selective catalytic reduction of NO by propylene with Cu-Al-Ce-PILC, and found a similar experimental phenomenon. However, the Al_xFe_y-PILC catalysts with different Al/Fe ratios prepared by Belver, et al. [10] exhibited the best SCR activity under oxygen-free conditions, and the catalytic performance dropped sharply with the addition of O_2. At present, the relevant research work on the effect of oxygen concentration on the HC-SCR reaction on the surface of pillared clay catalysts is not perfect, and the research on the effect mechanism is rarely reported in the literature.

In this paper, Fe-PCH catalyst was prepared with montmorillonite as parent clay and Fe ion as active metal, and the catalytic performance of Fe-PCH catalyst for C_3H_6-SCR under different oxygen concentrations was studied. Through the in-situ DRIFTS technology, the adsorbed species and reaction intermediates on the surface of the Fe-PCH catalyst during the reaction process was studied and the influencing mechanism of O_2 on the catalytic reactivity of Fe-PCH was

analyzed. On this basis, the reaction pathway of C_3H_6-SCR on the catalyst surface was proposed.

Experimental

Praparation of the Catalysts

Synthesis of PCH carrier: The raw material for synthesizing PCH carrier is K10 montmorillonite (Sinopharm Chemical Reagent, China). The clay particle size is less than or equal to 2μm, and the cation exchange capacity (CEC) is 102 meq/100g. First, the montmorillonite raw material is sodium treated. Then sodium montmorillonite (2g) was added to the surfactant solution (hexadecyltrimethylammonium chloride, 0.1M, 100ml) and stirred at 60 °C for 24h. Then, the clay was separated from the solution and washed with deionized water to pH 7. Next, add 2g of modified clay to neutral amine (dodecylamine) and organosilicon source (tetraethylorthosilicate-TEOS), the molar ratio of each substance is: modified clay/dodecylamine/TEOS=1 /20/150. After the mixture was continuously stirred at room temperature for 12 h, the modified clay material was separated from the solution and dried. Finally, PCHs materials were obtained by calcining at 600°C for 6 h in a muffle furnace.

Synthesis of Fe-PCH catalyst: The Fe-PCH catalyst was prepared by impregnation method. The process was as follows: 1.5g PCH carrier (about 5 cm^3 in volume) was added to 10 mL $Fe(NO_3)_3 \cdot 9H_2O$ solution with a concentration of 0.27 mol/L. The mixture was sonicated for 12 h and then placed in a 60°C water bath to evaporate to dryness. The samples were dried in a drying oven at 80°C for 12h, and finally placed in a muffle furnace, and calcined at 500°C for 3h to obtain Fe-PCH catalysts. The iron loading of the Fe-PCH catalyst was 8.4 wt%. .

Characterization of Basic Physicochemical Properties

The microscopic morphological characteristics of the catalysts were observed by transmission electron microscopy (TEM) (model JEM-2100F) with an accelerating voltage of 100 kV. The microporous characteristics of the catalyst were characterized by N_2 adsorption-desorption. The instrument used the ASAP-2460 adsorption instrument of Micromeritics. The detection results were calculated by BET equation and BJH model to obtain the specific surface area, pore volume and average pore size. The valence state distribution of each element on the catalyst surface can be analyzed by X-ray photoelectron spectroscopy (XPS) using a Thermo Escalab 250Xi spectrometer with Al-Kα excitation light source.

Su Y, et al. Effect of O_2 on Selective Catalytic Reduction of NO by C_3H_6 over Fe Catalysts Supported on Porous Clay Heterostructures (Fe-PCH). Pet Petro Chem Eng J 2022, 6(3): 000309.

Copyright© Su Y, et al.

SCR-C$_3$H$_6$ Activity

A fixed-bed microreactor was used to evaluate the SCR performance, and a Fourier transform infrared spectrometer (Thermo Nicolet IS10, thermoFisher, USA) was used to monitor the gas components online. The reaction gas composition is 0.1% C$_3$H$_6$, 0.1% NO, 0~10% O$_2$, N$_2$ balance, total flow 100ml/min. The diameter of the fixed bed reactor is 6 mm, the catalyst dosage is 400 mg, and the corresponding GHSV space velocity is 15000 h^{-1}. Before the start of the experiment, the residual air in the catalyst pores was removed by pretreatment in N$_2$ atmosphere at 300°C for 1 h.

The NO conversion and N$_2$ selectivity were calculated as follows:

$$NO\,conversion(\%) = \frac{[NO]_{in} - [NO]_{out}}{[NO]_{in}} \times 100\%$$

$$N_2\,selectivity\,(\%) = \frac{[NO]_{in} - [NO]_{out} - [NO_2]_{out} - 2[N_2O]_{out}}{[NO]_{in} - [NO]_{out}} \times 100\%$$

Where [NO], [NO$_2$] and [N$_2$O] are the volume fraction of the NO, NO$_2$ and N$_2$O respectively, the subscripts 'in' and 'out' stands for the values at inlet and outlet of the reactor respectively, ppm or %.

In situ DRIFTS studies

The intermediates generated during the reaction were investigated in situ by diffuse reflectance Fourier transform infrared spectrometer (DRIFTS) (Nicolet IS 50). Before the test, 50 mg of the catalyst sample was placed in the in-situ cell of the DRIFTS spectrometer and pretreated for 1 h at 500°C in an N$_2$ atmosphere to remove impurities adsorbed on the catalyst surface. During the experiment, the components of the reacting gas introduced were 0.1% C$_3$H$_6$, 0.1% NO and different concentrations of O$_2$, N$_2$ to be balanced, the total gas flow was 20 mL/min, and the reaction space velocity was 18000 h^{-1}.

Results and Discussion

C$_3$H$_6$-SCR Catalytic Reactivity

Figure 1 shows the test results of the C$_3$H$_6$-SCR catalytic activity on the Fe-PCH catalyst surface under different oxygen concentrations. As reported by Valverde, et al. [18], the critical oxygen concentration ([O$_2$]$_{crit}$) can be defined as the minimum oxygen concentration required for complete oxidation of propylene. It can be seen from Figure 1b that [O$_2$]$_{crit}$ is about 0.8% under the conditions studied in this paper.
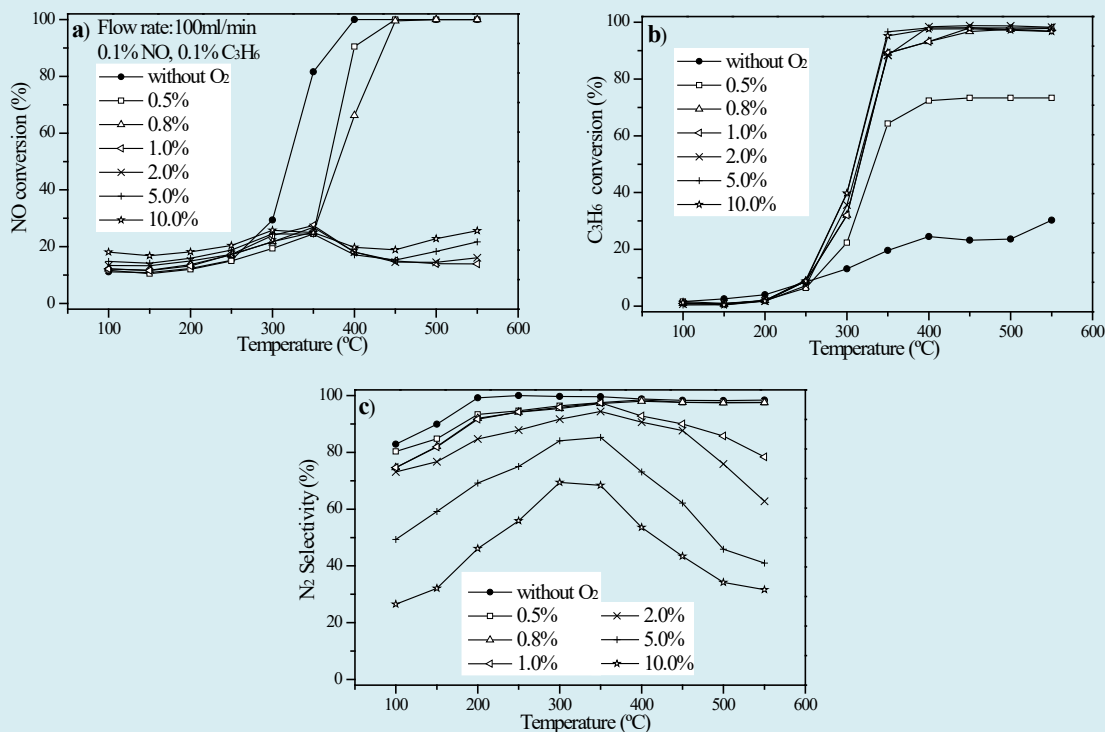

Figure 1: Influence of the O$_2$ concentration on C$_3$H$_6$-SCR over Fe-PCH catalysts: (a) NO conversion; (b) C$_3$H$_6$ conversion; (c) N$_2$ selectivity. Reactive condition: 0.1% NO, 0.1% C$_3$H$_6$, N$_2$ balance and GHSV=15000h^{-1}.

Su Y, et al. Effect of O$_2$ on Selective Catalytic Reduction of NO by C$_3$H$_6$ over Fe Catalysts Supported on Porous Clay Heterostructures (Fe-PCH). Pet Petro Chem Eng J 2022, 6(3): 000309.

Copyright© Su Y, et al.

As shown in Figure 1a, in the absence of oxygen supply, the Fe-PCH catalyst exhibits the best catalytic activity, and the NO conversion rate can reach 100% at 400 °C. When the oxygen concentration is increased in the range lower than $[O_2]_{crit}$, the catalytic activity gradually decreases, but the maximum NO conversion rate can still reach 100%. When the oxygen concentration is higher than $[O_2]_{crit}$, the selective catalytic reduction of NO activity on the catalyst surface drops sharply, and the maximum NO conversion rate drops to 20%-30%. However, at this time, the conversion rate of C_3H_6 has reached more than 90% at 350°C. This indicates that on the surface of Fe-PCH catalyst, propylene is preferentially combusted with O_2 to be consumed. When the oxygen concentration is lower than $[O_2]_{crit}$, the remaining propylene can further react with NO to generate N_2. However, when the oxygen concentration is higher than $[O_2]_{crit}$, only a small amount of C_3H_6 involves in the reduction reaction with NO. In addition, it can be seen from Figure 1c that with the increase of oxygen concentration, the N_2 selectivity gradually decreases, which is due to the oxidation of unreduced NO_2 by O_2 to generate a large amount of NO_2. In the range of 200~550°C, no by-product N_2O was detected.

TEM Characterization

Transmission electron microscopy (TEM) images can clearly observe the microscopic features of the catalyst surface. As shown in Figure 2, the Fe-PCH catalyst has a lamellar structure, and a three-dimensional pore structure is formed between the layers after being pillared by organic intercalation. The $\alpha\text{-Fe}_2O_3$ nanorods supported on the catalyst surface are the main active species in the process of C_3H_6-SCR catalytic reaction, and the crystal structure of this species corresponds to JCPDS card 33-0664. Its high-resolution image HRTEM (Figure 2c) shows that the interplanar spacings of the $\alpha\text{-Fe}_2O_3$ crystal surface are 0.185 nm and 0.272 nm, respectively, and the electron diffraction pattern is selected to analyze SADP (Figure 2d) on the (024) and (104) crystal planes, respectively. The exposed (104) crystal face of the $\alpha\text{-Fe}_2O_3$ nanorod crystal surface has a higher +3 valence Fe atomic density [20], which is conducive to the chemical adsorption of NO molecules [21], thereby improving the SCR reactivity.
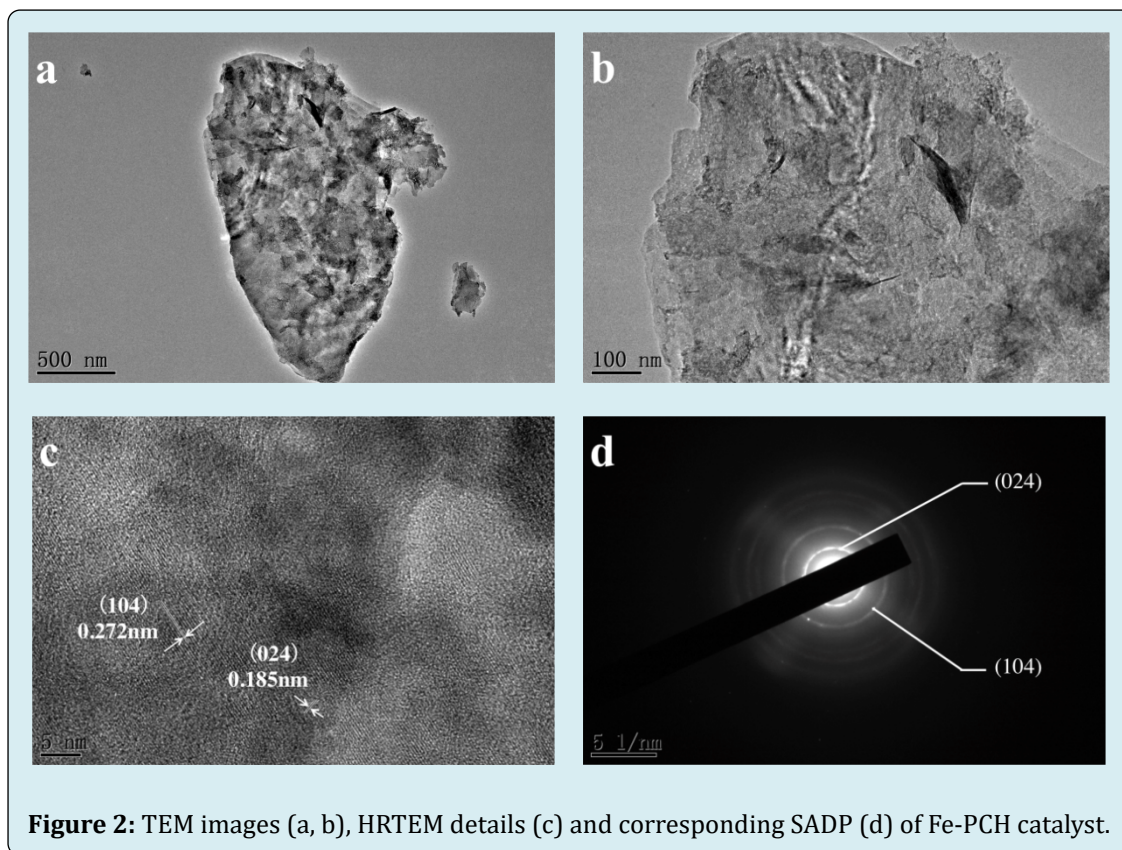

Figure 2: TEM images (a, b), HRTEM details (c) and corresponding SADP (d) of Fe-PCH catalyst.

N_2 Adsorption/Desorption

The pore characteristics of the catalysts can be detected by N_2 adsorption/desorption. The N_2 adsorption/desorption curves of the Fe-PCH catalyst sample and the original montmorillonite are shown in Figure 3, and the corresponding specific surface area, pore volume and pore size results are shown in Table 1.
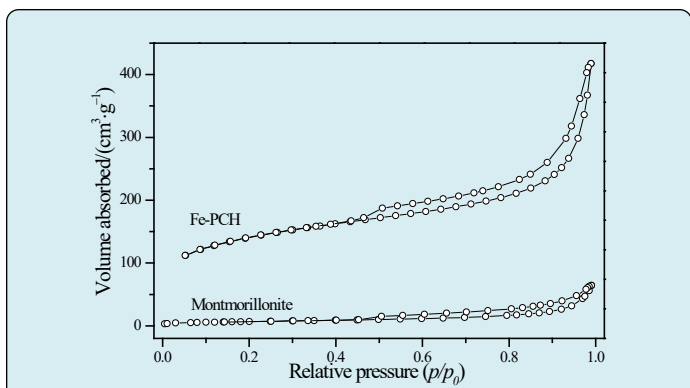
Su Y, et al. Effect of O_2 on Selective Catalytic Reduction of NO by C_3H_6 over Fe Catalysts Supported on Porous Clay Heterostructures (Fe-PCH). Pet Petro Chem Eng J 2022, 6(3): 000309.

Copyright© Su Y, et al.

Figure 3: Comparison of adsorption and desorption curves of Fe-PCH catalyst and parent clay montmorillonite.

The original N_2 adsorption capacity and specific surface area of montmorillonite were lower, and its N_2 adsorption isotherm belonged to IV type, and the hysteresis loop corresponds to H4 type. This shows that the mesoporous structure in the original montmorillonite is mainly formed by the irregular accumulation of lamellae [22]. The Fe-PCH catalyst has a large amount of N_2 adsorption, the adsorption isotherm belongs to the IV type, the hysteresis loop corresponds to the H3 type, and the corresponding specific surface area and pore volume value increase significantly. This is because the silica column is between the montmorillonite layers. Column support, so as to form an open cylindrical channel structure in the interlayer slot corridor area [1].

Samples	Specific Surface area/(m^2g^{-1})	Pore Volume/(cm^3g^{-1})	Pore Size/nm
Fe-PCH	470.6	0.64	5.45
Montmorillonite	24.2	0.1	16.44

Table 1: Specific surface area, pore volume and pore size of Fe-PCH catalyst and parent clay montmorillonite.

On the other hand, the average pore size of Fe-PCH material decreases, indicating that the pore structure of montmorillonite becomes regular and orderly after organic intercalation pillaring, which is conducive to the uniform dispersion of active components on the catalyst surface, thereby exposing more multiple active sites. In addition, in the range of $P/P_0=0.05-0.2$, the N_2 adsorption curve of Fe-PCH catalyst gradually increased, indicating that the material contains ultra-micropore and small mesoporous structure [16], which is helpful for the physical properties of reacting gas molecules adsorption process.

XPS Characterization

XPS characterization can further analyze the element valence and chemical properties of the catalyst surface active components. The XPS spectrum of Fe element on the surface of Fe-PCH catalyst and its peak fitting analysis results are shown in Figure 4a. Among them, the fitting separation peaks of Fe 2p3/2 peak are located at 710.88eV, 713.08eV and 714.88eV, respectively, and the satellite peak of Fe 2p3/2 is located at 718.18eV, which is consistent with the peak separation results of α-Fe_2O_3 species in the literature Li WG, et al. [23].
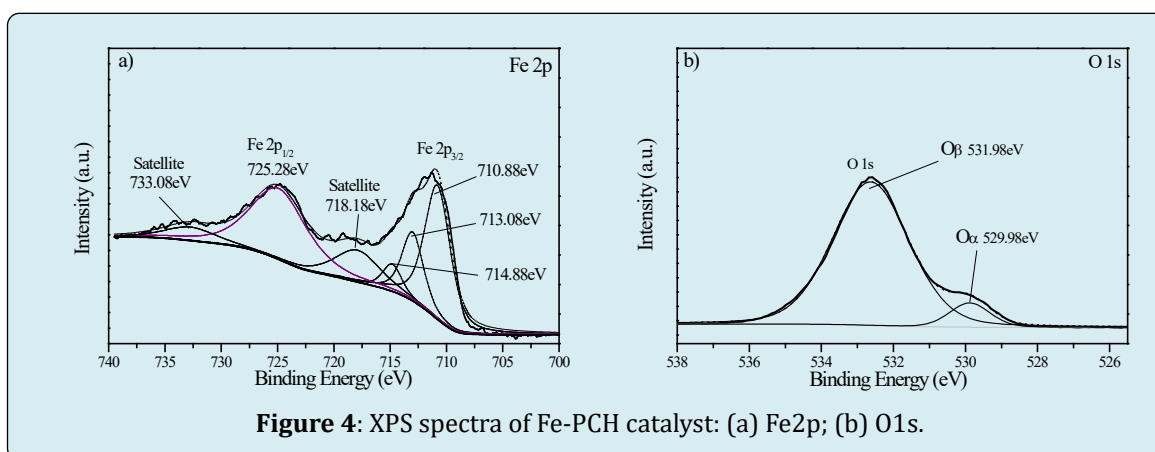

Figure 4: XPS spectra of Fe-PCH catalyst: (a) Fe2p; (b) O1s.

The XPS spectrum of O 1s in Figure 4b can be fitted to two sub-peaks. The sub-peak located at the binding energy of 529.98 eV represents the lattice oxygen O^{2-} (denoted as O_α), and the sub-peak located at 531.98 eV corresponds to the adsorbed oxygen species (denoted as O_β). The lattice oxygen species $O\alpha$ is beneficial to the activation of C_3H_6 on the catalyst surface [24], thereby improving the SCR activity of the catalyst. However, the adsorbed oxygen species O_β will

promote the complete oxidation of C_3H_6 by O_2 to CO_2 [25].

In situ DRIFTS Spectra

The in-situ DRIFTS technique can be used to detect the adsorbed species and reaction intermediates on the catalyst surface during the reaction. Combined with the test results of C_3H_6-SCR performance of Fe-PCH catalysts under different oxygen concentrations, three conditions of no oxygen, lower than $[O_2]_{crit}$ (0.5% O_2) and higher than $[O_2]_{crit}$ (2% O_2) were selected to study the adsorption species of C_3H_6 and NO on Fe-PCH catalyst surface. The reaction temperature is 300°C. Figure 5 shows the DRIFTS spectra of C_3H_6 adsorbed species on the Fe-PCH catalyst surface under different oxygen concentrations.
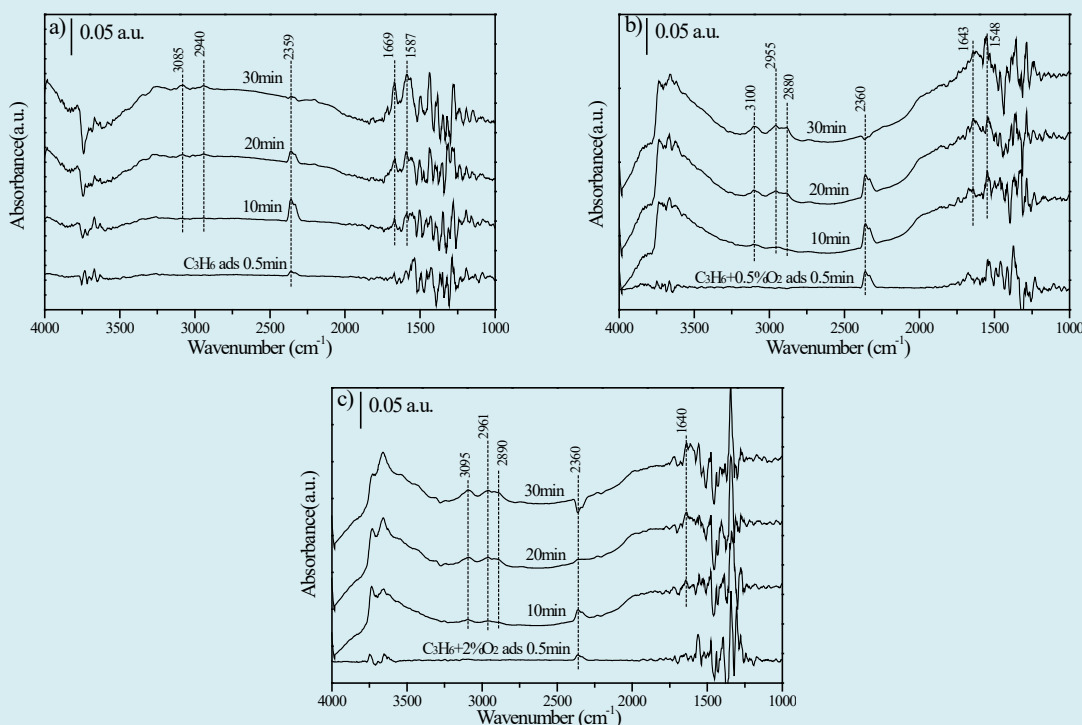

Figure 5: In situ DRIFTS results of C_3H_6 adsorbed species under (a) without oxygen; (b) 0.5% O_2; (c) 2% O_2 over Fe-PCH catalyst at 300°C. Reactive condition: 0.1% C_3H_6, N_2 balance and GHSV=18000h^{-1}.

As shown in Figure 5, the characteristic peaks at 3100-2800 cm^{-1} correspond to the asymmetric stretching of C-H bonds [26]. The characteristic peak around 1650cm^{-1} corresponds to the stretching vibration of C=C bond [27]. The characteristic peak near 1550cm^{-1} corresponds to the C-H bond vibration [27]. In addition, the characteristic peak at 2360cm^{-1} broadband represents CO^2 species [28]. At the beginning of the adsorption process (0.5min), the spectra were all in a horizontal state, and there were no obvious characteristic peaks except for a small amount of CO_2 gas. With the progress of the adsorption process, the intensity of the characteristic peaks of the adsorbed species on the catalyst surface gradually increased. It can be found from the figure that with the increase of oxygen concentration, the characteristic peak intensity at the broadband of 3100-2800 cm^{-1} gradually increases, which indicates that the addition of O_2 is beneficial to the activation process of C_3H_6 on the surface of Fe-PCH catalyst. According to the interfacial mechanism of hydrocarbon-catalyzed oxidation (Mars-van-Krevelen), lattice oxygen O^{2-} species on the surface of Fe-PCH catalyst can promote the activation process of propylene. The active lattice oxygen is consumed by hydrocarbons to form anion vacancies, and then the process of regenerating lattice oxygen by adsorption of gaseous O_2 on the surface.

Figure 6 shows the DRIFTS spectra of C_3H_6+NO adsorbed species on the Fe-PCH catalyst surface under different oxygen concentrations. The catalyst was first adsorbed in the C_3H_6 atmosphere with different oxygen concentrations for 30 min, and then NO was introduced. It can be found from the figure that a distinct characteristic peak appears at 2235 cm^{-1}, which corresponds to the important intermediate isocyanate species (R-NCO) in the C_3H6-SCR reaction [24]. As the oxygen concentration increased, the characteristic peak intensity of the R-NCO species gradually weakened, indicating that the formation of this species was inhibited.
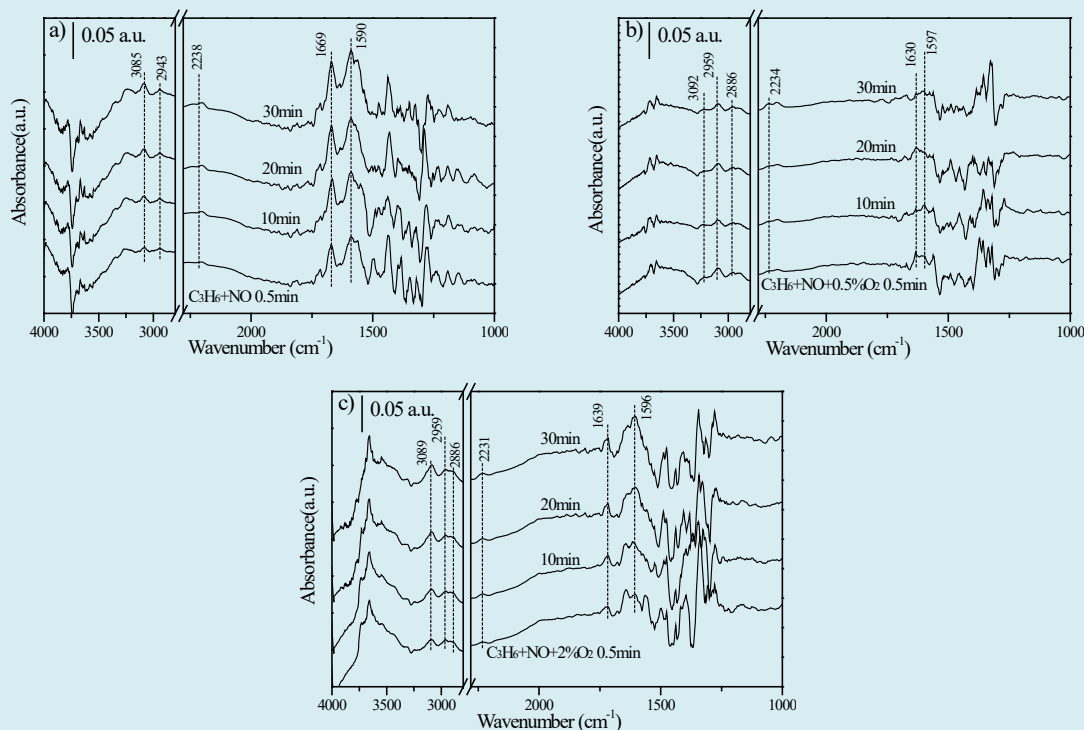
Su Y, et al. Effect of O_2 on Selective Catalytic Reduction of NO by C_3H_6 over Fe Catalysts Supported on Porous Clay Heterostructures (Fe-PCH). Pet Petro Chem Eng J 2022, 6(3): 000309.

Copyright© Su Y, et al.

Figure 6: In situ DRIFTS results of C_3H_6+NO adsorbed species under (a) without oxygen; (b) 0.5% O_2; (c) 2% O_2 over Fe-PCH catalyst at 300°C. Reactive condition: 0.1% C_3H_6, 0.1% NO, N_2 balance and GHSV=18000h^{-1}.

The effect of oxygen concentration on the C_3H_6-SCR activity on the Fe-PCH catalyst surface can be further analyzed in combination with the in-situ DRIFTS spectra of the C_3H_6 + NO + O_2 adsorbed species, as shown in Figure 7.
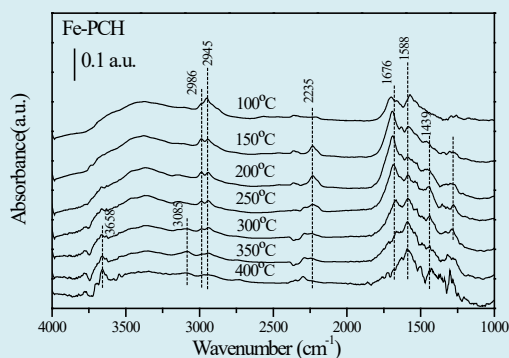

Figure 7: In situ DRIFTS spectra of C_3H_6+NO+O_2 adsorbed species under different temperatures over Fe-PCH catalyst. Reactive condition: 0.1% C_3H_6, 0.1% NO, 2% O_2, N_2 balance and GHSV=18000h^{-1}.

The characteristic peaks at 1588cm^{-1} and 1439cm^{-1} correspond to $C_xH_yO_z$ and acetate (CH_3COO-) species, respectively [26,27]. The characteristic peak at 1676cm^{-1}

corresponds to the nitrogen-containing organic intermediate (R-NO$_2$) [27]. In addition, the characteristic peak at 3658 cm^{-1} may be generated by the shear bending vibration of the O-H bond [28]. The redox mechanism of selective catalytic reduction of NO by hydrocarbons is that hydrocarbons are activated and oxidized on the catalyst surface to $C_xH_yO_z$(ads) (or acetate) species, and then react with NO_x(ads) (or nitrate) species to form nitrogen-containing species Organic intermediates, which are converted into species such as isocyanates on the catalyst surface, and finally obtain the products N_2, CO_2 and H_2O. Oxygen inhibits the formation of isocyanate species on the surface of Fe-PCH catalysts, thereby reducing their catalytic activity for C_3H_6-SCR.

Reaction Mechanism

Oxygen is required to activate the oxidation of hydrocarbons in the reaction pathway of the redox mechanism of HC-SCR. It was found that the pillared clay catalyst with isolated Cu^{2+} as the active center has almost no HC-SCR catalytic activity under anaerobic conditions [18]. However, Fe-PCH catalysts showed better C_3H_6-SCR catalytic performance under anaerobic conditions, and Zhou [24], Belver [10] also found similar phenomena. Therefore, the process of adsorption and decomposition of NO should still exist on the surface of Fe-PCH catalyst.

Su Y, et al. Effect of O_2 on Selective Catalytic Reduction of NO by C_3H_6 over Fe Catalysts Supported on Porous Clay Heterostructures (Fe-PCH). Pet Petro Chem Eng J 2022, 6(3): 000309.

Copyright© Su Y, et al.

The reaction mechanism is shown in Figure 8. In the adsorption decomposition path [29], NO is decomposed into adsorbed nitrogen atoms (N_{ad}) and adsorbed oxygen atoms (O_{ad}) on the surface of Fe-PCH catalyst, and the two N_{ad} can combine to generate N_2. Part of O_{ad} can oxidize C_3H_6 to generate $C_xH_yO_z$ or CO_2 and H_2O, and O_{ad} can also generate new lattice oxygen through oxygen migration to participate in the redox pathway of SCR.
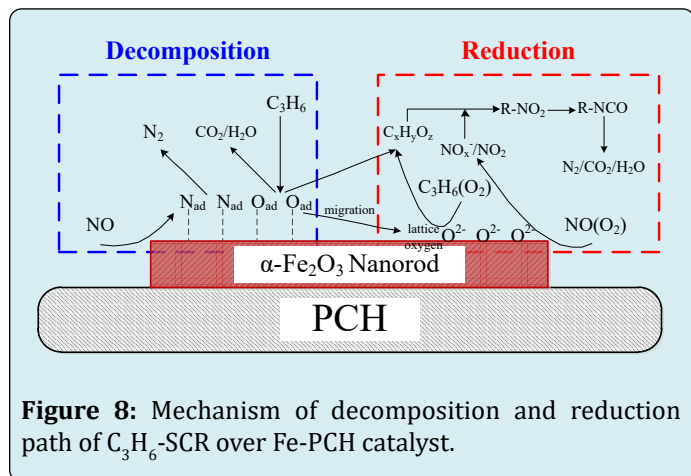

Figure 8: Mechanism of decomposition and reduction path of C_3H_6-SCR over Fe-PCH catalyst.

Conclusion

1. Under anaerobic conditions, the catalytic performance is the best, and the NO conversion rate can reach 100% at 400 °C. When the oxygen concentration is lower than $[O_2]_{crit}$, the catalytic activity of Fe-PCH gradually decreases with the increase of oxygen concentration. When the oxygen concentration is higher than $[O_2]_{crit}$, the catalytic performance drops sharply.

2. The characterization results of TEM, BET and XPS show that the Fe-PCH catalyst has a relatively regular pore structure, the α-Fe_2O_3 nanorods supported on the surface are the main active components, and the exposed (104) crystal surface of the Fe_2O_3 crystal surface is conducive to the adsorption of NO and exists The lattice oxygen species are favorable for the activation of propylene.

3. The results of in situ DRIFTS spectra showed that the increase of oxygen concentration favored the activation oxidation of propylene, but inhibited the formation of reaction intermediate isocyanate species, thereby reducing the reactivity of Fe-PCH catalyst. The C_3H_6-SCR reaction process on the surface of Fe-PCH catalyst should have both the adsorption and decomposition path and the redox path of NO.

References

1. Mrad R, Aissat A, Cousin R, Courcot D, Siffert S, et al. (2015) Catalysts for NOx selective catalytic reduction by hydrocarbons (HC-SCR). Appl Catal A Gen 504: 542-548.

2. More PM (2017) Effect of active component addition and support modification on catalytic activity of Ag/Al2O3 for the selective catalytic reduction of NOx by hydrocarbon – a review. J Environ Manage 188(1): 43-48.

3. Yang RT, Li WB (1995) Ion-exchanged pillared clays: a new class of catalysts for selective catalytic reduction of NO by hydrocarbons and by ammonia. J Catal 155(2): 414-417.

4. Lu G, Li X, Qu Z, Zhao Q, Zhao L, Chen G, et al. (2011) Copper-ion exchanged Ti-pillared clays for selective catalytic reduction of NO by propylene. Chem Eng J 168(3): 1128-1133.

5. Zhang X, Hu X, Liu S, Chen Y, Jin S, et al. (2022) MnOx-pillared rectorite prepared by in situ deposition as efficient catalysts for low-temperature NH3-SCR: The influences of manganese (II) precursors. Journal of Environmental Chemical Engineering 10(2): 107318.

6. Su Y, Wen N, Cheng J, Deng W, Zhou H, et al. (2020) Experimental study on the SCR-C3H6 over Cu-Fe/Al-PILC catalysts: Catalytic performance, characterization and the mechanism. Ind Eng Chem Res 59(33): 14776-14788.

7. Wen N, Dong S, Su Y, Deng W, Zhao B, et al. (2020) Effect of Synthesis parameters on catalytic performance of Fe/Ti-PILC catalysts for SCR-C3H6 and in situ DRIFTS study. Journal of Environmental Chemical Engineering 8(6): 104555.

8. Cheng J, Ye Q, Li C, Cheng S, Kang T, et al. (2020) Ceria-modified Al-Mn-pillared clay catalysts for the selective catalytic reduction of NO with NH3 at low temperatures. Asia-Pacific Journal of Chemical Engineering 15(3): e2439.

9. Zhang XW, Su YX, Cheng JH, Lin R, Wen NN, et al. (2019) Effect of Ag on deNOx performance of SCR-C3H6 over Fe/Al-PILC catalysts. Journal of Fuel Chemistry and Technology 47(11): 1368-1378.

10. Cheng JH, Su YX, Li QC, Wen NN, Deng WY, et al. (2019) Experimental study on selective catalytic reduction of NO by C3H6 over Cu-Fe-PILC. Chinese Journal of Inorganic Chemistry 35(12): 2291-2300.

11. Han Z, Yu Q, Xie H, Liu K, Qin Q, et al. (2018) Fabrication of manganese-based Zr-Fe polymeric pillared interlayered montmorillonite for low-temperature selective catalytic reduction of NOx by NH3 in the metallurgical sintering flue gas. Environ Sci Pollut Res Int 25(32): 32122-32129.

Su Y, et al. Effect of O_2 on Selective Catalytic Reduction of NO by C_3H_6 over Fe Catalysts Supported on Porous Clay Heterostructures (Fe-PCH). Pet Petro Chem Eng J 2022, 6(3): 000309.

Copyright© Su Y, et al.

12. Cheng J, Song Y, Ye Q, Cheng SY, Kang TF, et al. (2018) A mechanistic investigation on the selective catalytic reduction of NO with ammonia over the V-Ce/Ti-PILC catalysts. Molecular Catalysis 445:111-123.

13. Qian WY, Su YX, Yang Xi, Yuan MH, Deng WY, et al. (2017) Experimental study on selective catalytic reduction of NO with propene over iron based catalysts supported on aluminum pillared clays. J Fuel Chem Technol 45(12): 1499-1507.

14. Dong SL, Su YX, Liu X, Li QC, Yuan MH, et al. (2018) Experimental study on selective catalytic reduction of NO by C3H6 over Fe/Ti-PILC catalysts. J Fuel Chem Technol 46(10): 1231-1239.

15. Li QC, Su YX, Dong SL, Yuan MH, Zhou H, et al. (2018) Fe-PILC for selective catalytic reduction of NO by propene under lean-burn conditions. J Fuel Chem Technol 46: 99-107.

16. Galarneau A, Barodawalla A, Pinnavala T (1995) Porous clay heterostructures formed by gallery-templated synthesis. Nature 374: 529-531.

17. Yuan M, Deng W, Dong S, Li Q, Zhao B, et al. (2018) Montmorillonite based porous clay heterostructures modified with Fe as catalysts for selective catalytic reduction of NO with propylene. Chem Eng J 353: 839-848.

18. Valverde JL, Lucas AD, Dorado F, Romero A, Garcia PB, et al. (2005) Influence of the operating parameters on the selective catalytic reduction of NO with hydrocarbons using Cu-ion-exchanged titanium-pillared interlayer clays (Ti-PILCs). Ind Eng Chem Res 44(9): 2955-2965.

19. Lin QC, Lin WM, Hao JM, Li JH (2006) Effect of reaction conditions on catalytic performance of Cu/Al-Ce-PILC for selective catalytic reduction of NO by propylene. Chinese J Catal 27: 69-74.

20. Lv B, Liu Z, Tian H, Wu D, Sun Y, et al. (2010) Single-crystalline dodecahedral and octodecahedral α-Fe2O3 particles synthesized by a fluoride anion–assisted hydrothermal method. Adv Funct Mater 20(22): 3987-3996.

21. Mou X, Zhang B, Li Y, Yao L, Wei X, et al. (2012) Rod-shaped Fe2O3 as an efficient catalyst for the selective reduction of nitrogen oxide by ammonia. Angew Chem Int Ed Engl 51(12): 2989-2993.

22. Mao H, Li B, Li X, Yue L, Liu Z, et al. (2010) Novel one-step synthesis route to ordered mesoporous silica-pillared clay using cationic-anionic mixed-gallery templates. Ind Eng Chem Res 49(2): 583-591.

23. Li WG, Li G, Jin CZ, Liu X, Wang JH, et al. (2015) One-step synthesis of nanorod-aggregated functional hierarchical iron-containing MFI zeolite microspheres. J Mater Chem A 3: 14786-14793.

24. Yuan M, Su Y, Deng W, Zhou H (2019) Porous clay heterostructures (PCHs) modified with copper ferrite spinel as catalyst for SCR of NO with C3H6. Chem Eng J 375: 122091.

25. Zhou H, Li K, Zhao B, Deng W, Su Y, et al. (2017) Surface properties and reactivity of Fe/Al2O3/cordierite catalysts for NO reduction by C2H6: Effects of calcination temperature. Chem Eng J 326: 737-744

26. Zhang F, Zhang S, Guan N, Schreier E, Richter M, et al. (2007) NO SCR with propane and propene on Co-based alumina catalysts prepared by co-precipitation. Appl Catal B Environ 73(3-4): 209-219.

27. Dorado F, Garxia PB, Lucas AD, Ramos MJ, Romero A, et al. (2010) Hydrocarbon selective catalytic reduction of NO over Cu/Fe-pillared clays: diffuse reflectance infrared spectroscopy studies. J Mol Catal A Chem 332(1-2): 45-52.

28. Zhou H (2016) NO reduction with light alkanes over iron and Fe-based catalysts [D]. Donghua University, Shanghai, China.

29. Burch R, Breen JP, Meunier FC (2002) A review of the selective reduction of NOx with hydrocarbons under lean-burn conditions with non-zeolitic oxide and platinum group metal catalysts. Appl Catal B Environ 39(4): 283-303.

Su Y, et al. Effect of O_2 on Selective Catalytic Reduction of NO by C_3H_6 over Fe Catalysts Supported on Porous Clay Heterostructures (Fe-PCH). Pet Petro Chem Eng J 2022, 6(3): 000309.

Copyright© Su Y, et al.